AGU PUBLICATIONS

JGR

Journal of Geophysical Research: Oceans

RESEARCH ARTICLE

10.1002/2017JC012861

Special Section:
The Southern Ocean Carbon and Climate Observations and Modeling (SOCCOM) Project: Technologies, Methods, and Early Results

# Evaluating Southern Ocean Carbon Eddy-Pump From Biogeochemical-Argo Floats

**Joan Llort[1,2,3], C. Langlais[3], R. Matear[2,3], S. Moreau[1,4], A. Lenton[3,5], and Peter G. Strutton[1,2,3]**

[1]Institute of Marine and Antarctic Sciences, University of Tasmania, Hobart, Tas, Australia, [2]Australian Research Council Centre of Excellence for Climate System Science, Hobart, Tas, Australia, [3]CSIRO Oceans and Atmosphere, Hobart, Tas, Australia, [4]Australian Research Council Antarctic Gateway Strategic Research Initiative, Hobart, Tas, Australia, [5]Antarctic Climate and Ecosystems CRC, Hobart, Tas, Australia

**Abstract** The vertical transport of surface water and carbon into ocean's interior, known as subduction, is one of the main mechanisms through which the ocean influences Earth's climate. New instrumental approaches have shown the occurrence of localized and intermittent subduction episodes associated with small-scale ocean circulation features. These studies also revealed the importance of such events for the export of organic matter, the so-called *eddy-pump*. However, the transient and localized nature of episodic subduction hindered its large-scale evaluation to date. In this work, we present an approach to detect subduction events at the scale of the Southern Ocean using measurements collected by biogeochemical autonomous floats (BGCArgo). We show how subduction events can be automatically identified as anomalies of spiciness and Apparent Oxygen Utilization (AOU) below the mixed layer. Using this methodology over more than 4,000 profiles, we detected 40 subduction events unevenly distributed across the Sothern Ocean. Events were more likely found in hot spots of eddy kinetic energy (EKE), downstream major bathymetric features. Moreover, the bio-optical measurements provided by BGCArgo allowed measuring the amount of Particulate Organic Carbon (POC) being subducted and assessing the contribution of these events to the total downward carbon flux at 100 m (EP100). We estimated that the eddy-pump represents less than 19% to the EP100 in the Southern Ocean, although we observed particularly strong events able to locally duplicate the EP100. This approach provides a novel perspective on where episodic subduction occurs that will be naturally improved as BGCArgo observations continue to increase.

**Plain Language Summary** The vertical transport of surface organic carbon into the deep ocean is a fundamental question in oceanography. This transport of carbon supports ocean ecosystems and influences the global climate. Recently, several studies have observed that vertical transport can occur as short-lived events. These events are the most efficient way to inject surface organic carbon into the ocean, yet they are extremely hard to observe. In this study, we used autonomous floats to capture them. The observations made by these floats during the last 3 years allowed us to map, for the first time, the spatial distribution of vertical transport events throughout the Southern Ocean. Interestingly, we found that these events were concentrated in regions where ocean currents interact with bathymetry. Moreover, our study provides an innovative approach to observe the episodic transport of carbon from autonomous floats.

**Key Points:**
- We use Argo floats equipped with biogeochemical sensors to detect subduction events in the Southern Ocean
- We found that events were concentrated in hot spots of high eddy activity, downstream major topographic features
- Our results suggest that the contribution of this mechanism to the biological carbon pump in the Southern Ocean might be lower than previously proposed

**Supporting Information:**
- Supporting Information S1
- Figure S1
- Figure S2
- Figure S3

**Correspondence to:**
J. Llort,
jllort@utas.edu.au

**Citation:**
Llort, J., Langlais, C., Matear, R., Moreau, S., Lenton, A., & Strutton, P. G. (2018). Evaluating Southern Ocean Carbon Eddy-Pump From Biogeochemical-Argo Floats. *Journal of Geophysical Research: Oceans*, *123*, 971–984. https://doi.org/10.1002/2017JC012861

Received 11 MAR 2017
Accepted 16 JAN 2018
Accepted article online 19 JAN 2018
Published online 6 FEB 2018



## 1. Introduction

Over the last decade, it has become increasingly clear that the unique and vigorous dynamics of the Southern Ocean give rise to a diversity of vertical transport pathways: from the largest to the smallest circulation scales (Rosso et al., 2014; Sabine et al., 2004; Sallée et al., 2012). Such pathways are the major mechanism through which the Southern Ocean influences climate, by transferring water between the surface and the ocean interior (Turner et al., 2009). The pathways that isolate surface waters below the upper mixed layer, through a process known as subduction (Williams, 2001), are particularly relevant for the Earth's climate because they extract heat and carbon from the atmosphere and store it in the ocean's interior (Sabine et al., 2004; Watson et al., 2014).

Climatologically, subduction results from the coupling of large-scale circulation and the seasonal cycle of the mixed-layer depth (MLD) (Lévy et al., 2013; Williams, 2001). In the places where this coupling occurs, large volumes of water are injected into the ocean. Recent advances in ocean modeling have highlighted the importance of small-scale ocean circulation on vertical exchanges and, particularly, on subduction (Koch-Larrouy et al., 2010; Spall, 1995; Xu et al., 2014) and ocean biogeochemistry (Klein & Lapeyre, 2009; McGillicuddy, 2016). This circulation is composed of eddies, fronts, and jets at scales of ~1–100 km, which we collectively refer in this paper as small-scale circulation. The influence of small-scale circulation on both the physical and the biological carbon oceanic pumps is highly localized and episodic, and therefore difficult to quantify from a climate perspective.

At the same time, technical improvements in instrumentation and new sampling strategies have allowed subduction events to be observed (Naveira Garabato et al., 2001; Xu et al., 2016). In particular, episodic subduction has been shown to contribute to the biological carbon pump transferring dissolved and particulate organic matter from the surface into the mesopelagic zone (Omand et al., 2015; Stukel et al., 2017a, 2017b; Ruiz et al., 2009). For instance, Omand et al. (2015) provided a model-based estimation suggesting that this mechanism, that they called the *eddy-pump*, may represent 50% of the total export of Particulate Organic Carbon (POC) in the North Atlantic, the Kuroshio extension and the Southern Ocean. More recently, Stukel and Ducklow (2017) estimated that the passive export of organic matter caused by vertical mixing and subduction (including episodic subduction) might represent 23% of total biological carbon pump in the Southern Ocean. To date, the observation of subduction events has been limited to a single occurrence and therefore the evaluation of their significance at the basin-scale is extremely difficult.

The aim of our work is to detect subduction events in the Southern Ocean, and provide a synoptic view of where they occur. To do so, we used measurements made by new observation platform: autonomous profiling floats equipped with biogeochemical sensors, referred to as biogeochemical-Argo floats, or BGCArgo hereafter. Our study provides the first basin-scale evaluation of episodic subduction events. Such evaluation is a critical first step to elucidating the contribution of subduction events to both mode-water formation and carbon export in the Southern Ocean, one of the most climate-relevant regions of the global ocean.

## 2. Data

### 2.1. Satellite Data

To identify the surface mesoscale circulation where floats profiled, daily maps of sea surface height (SSH) and derived geostrophic velocities ($V_g$) were created from satellite absolute dynamical topography (ADT) estimations (http://www.aviso.altimetry.fr/en/data/products/sea-surface-height-products/global/madt-h-uv.html) using the delayed time (DT)—*all satellite* daily products between 2006 and 2015. Eddy kinetic energy (EKE) was also computed as $EKE = \frac{1}{2}\sqrt{u'^2+v'^2}$, where $u' = u-\bar{u}$. $u$ and $v$ are the daily data, and $\bar{u}$, $\bar{v}$ represent 10 year averages.

### 2.2. Biogeochemical-Argo Floats

#### 2.2.1. Float Data

SOCCOM (40 floats and 2,751 profiles) and SOCLIM-remOcean (17 floats and 8,100 profiles) programs deployed all floats used in this work. These two programs are part of an international effort on deploying BGCArgo floats around the global ocean and in the Southern Ocean in particular (Claustre & Johnson, 2016). Although data are currently distributed through different platforms, the BGCArgo website (http://biogeochemical-Argo.org/index.php) gathers together updated information on the ensemble of the BGCArgo fleet, as well as the projects that deployed them. These floats follow the same sampling procedure as traditional Argo floats, with water column samplings of the first 1,500 m of the ocean (called stations hereafter) scheduled between standby periods of 5–10 days. During the standby phase, floats are "parked" at 1,000 m depth. Ollitrault and Rannou (2013) showed that, globally, the statistical distribution of surface velocities estimated from Argo floats is very similar to the distribution of velocities at the parking depth (Figures 17–20 in their manuscript). This is especially true in the Southern Ocean, where the circulation has been described as equivalent barotropic (Gille et al., 2007; Killworth & Hughes, 2002). An equivalent barotropic circulation basically implies that the strength of the current might

change with depth (weaker as depth increases) but the orientation does not change. Therefore, Argo and BGCArgo can be interpreted as "quasi-Lagrangian" because floats follow well ocean mesoscale circulation lasting more than 1 week; yet they cannot follow shorter and smaller features such the ones associated to submesocale circulation.

In addition to the standard Argo CTD sensors, BGCArgo are equipped with a number of biogeochemical sensors such as, fluorescence, nitrate concentration, pH or optical backscatter (for details, see the SOCLIM http://soclim.com/instrumentation-en.php and SOCCOM https://soccom.princeton.edu/content/float-data websites). For our study, we used measurements of temperature, salinity, oxygen, fluorescence, and optical backscatter. The latter is used as a proxy for the concentration of particles. In order to focus on open Southern Ocean waters, we discarded all profiles north of 30°S and south of 65°S. We also filtered coastal waters and intrusions of tropical waters by discarding profiles with surface salinities higher than 35.0 psu. In total, the database used in our study contained 4,336 profiles collected between 2012 and November 2016.

#### 2.2.2. Data Preparation and Derived Variables

All variables were vertically smoothed applying a 3 bin running mean to reduce noise. Each depth bin is approximately 3–5 m so this is equivalent to a 9–15 m smoothing. Optical backscatter data ($b_{bp}$) were smoothed with a 7 bin running mean, equivalent to a vertical interval of 20–35 m, to eliminate spikes (Briggs et al., 2011). The smoothed $b_{bp}$ signal was then used to estimate POC concentration following Haëntjens et al. (2017).

Temperature and salinity data were used to estimate the saturation oxygen concentration (Osat) at each point (Garcia & Gordon, 1992). The difference between Osat and the observed Dissolved Oxygen (DO) is defined as the Apparent Oxygen Utilization (AOU), and is a proxy for water mass age (Sarmiento & Gruber, 2006). In the ocean, oxygen concentration at the surface is assumed to be equal to or slightly higher than its saturated value, hence surface AOU is close to 0 or slightly positive. When a water mass becomes isolated from the surface, it loses oxygen due to heterotrophic respiration, leading to an increase in AOU. Low AOU values at depth are indicative of recent water exchange with the surface. The main benefit of calculating AOU rather than simply using DO is that the former does not depend on the temperature of the water mass. In the Southern Ocean, AOU surface values range between 0 and 20 $\mu$mol $L^{-1}$, with a strong latitudinal gradient around 55°S (supporting information Figure S1). This gradient, which propagates to 1,000 m, is due to the mixing of the upwelled high AOU deep waters south of the Polar Front with the sub-Antarctic low AOU waters north of the Polar Front.

In our study, we also used a physical variable called spiciness (Flament, 2002). Spiciness allows differentiating water masses with distinct thermohaline properties but similar density. Although several definitions have been proposed for Spiciness (Flament, 2002; Huan, 2011; McDougall & Krzysik, 2015), here we used the definition and symbol ($\pi$) proposed by Flament (2002), for consistency with Omand et al. (2015). In the Southern Ocean, spiciness has a strong gradient in the upper ocean with values ranging $-1$ to 5 kg/$m^3$ (supporting information Figure S1).

### 2.3. Spatial and Vertical Data Distribution

Profiles from BGCArgo floats were unevenly distributed over the Southern Ocean (Figure 1). Most of them were located between the Polar Front (PF) and the Sub-Antarctic Front (SAF). In the Indian and Pacific sectors, a significant number of profiles were found north of the Sub-Tropical Front (STF). The PF appeared as a dynamical barrier for most of the floats and very few profiles were found south of the PF. Large gaps of data persist in the Eastern Pacific sector, Drake Passage, and Atlantic sector, where very few floats have been deployed yet.

The highest density of profiles (more than 30 profiles per 0.5°) was found in waters surrounding Kerguelen Plateau and south of Tasmania. The Indian, Australian, and west-central Pacific sectors were covered with an average density of five profiles per 0.5°. Most floats sampled the water column down to 1,000 m. However, the vertical resolution of biogeochemical measurements varied with depth and by deploying program. SOCCOM floats sampled the first 100 m at a 5 m resolution, between 100 and 400 m at a 10 m resolution and depths below 400 m at a 50 m resolution. SOCLIM-remOcean floats generally sampled at a 10 m resolution from surface to 1,000 m deep. The sampling frequency also varied among deploying programs and floats. Most floats profiled every 9–10 days. However, a significant number of floats, mostly from the SOCLIM-remOcean program, sampled at faster rates, every 3–5 days.

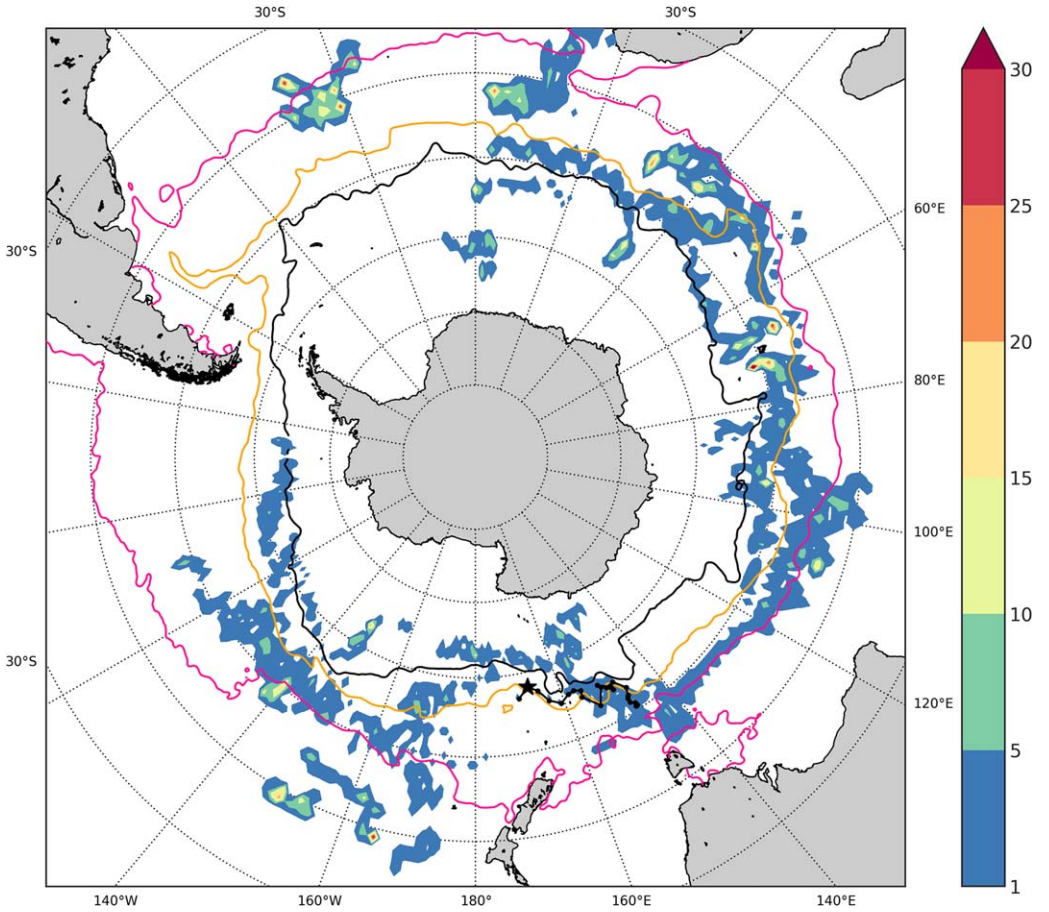


**Figure 1.** Spatial density map of oxygen profiles per 0.5° as of 28 November 2016. Black-dotted line represents the trajectory of float WMO59046977, black dots indicate profiles location and black star marks the location of profile number 27 (detailed in Figure 3). Pink, orange, and black solid lines represent the climatological position of the STF, the SAF and, PF respectively, as defined in Venables et al. (2012).

### 2.4. Detection Method

Omand et al. (2015) showed that when a surface water parcel is injected below the mixed layer it carries anomalous values of DO (and AOU), spiciness, and POC into the mesopelagic zone. Such anomalies are coherently advected and observed in vertical profiles at the vicinity of the injection. BGCArgo floats data provide estimates of AOU, spiciness, and POC (Figure 2) at the same vertical resolution used by Omand et al. (2015) and Xu et al. (2016). While this database has the potential for opportunistic observations of subduction events, BGCArgo data also present some challenges that need to be taken into account. The main limitation of the BGCArgo database is that it provides vertical profiles of isolated water columns. The spatial separation between two consecutive profiles is of the order of 100 km (Ollitrault & Rannou, 2013), even more in regions of high-speed surface currents (>50 cm/s). The Lagrangian time series measured by a particular float (Figure 2) are then influenced by both the spatial and temporal variability. Moreover, small-scale subduction occurs as a three-dimensional water pathway that has only been observed by heavily instrumented studies covering small oceanic domains (Omand et al., 2015; Stukel et al., 2017a, 2017b; Xu et al., 2016), and thus with high horizontal resolution. This 3-D pathway, that originates in the upper mixed layer and penetrates into the mesopelagic zone or deeper, transports water with surface properties along an isopycnal layer. BGCArgo data cannot fully capture the pathway of subducted water, nor to detect the strong horizontal density gradients at the surface that eventually lead to subduction. However, when a BGCArgo float passes through a parcel of injected water it captures coherent anomalous features below the mixed layer that can be associated to a subduction event occurring at the vicinity. Thus, our hypothesis is that the occurrence of episodic subduction events can be evaluated from the opportunistic measurements of anomalies across the subduction pathways.

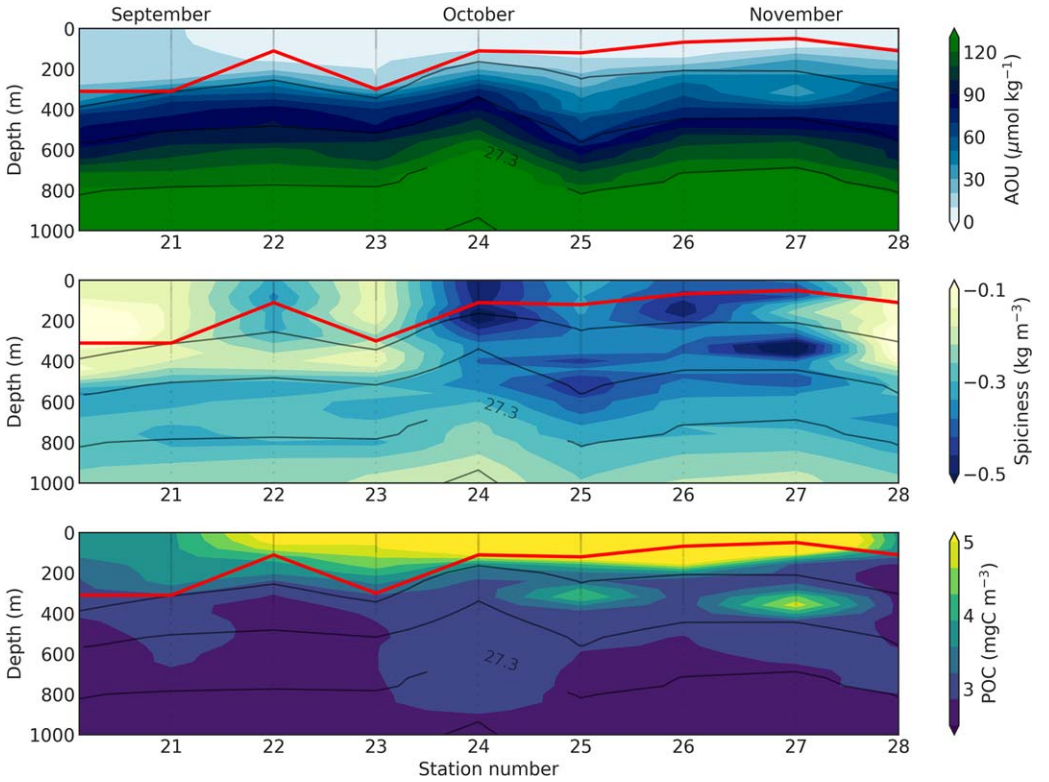


**Figure 2.** Lagrangian time series of float WMO5904677 observations between profiles number 20 and 28 (5 September to 25 November 2016), (a) AOU derived from dissolved oxygen, temperature, and salinity observations. (b) Spiciness derived from T and S; (c) POC estimated from optical backscattering measurements (see text for details).

BGCArgo profiles provide a unique database where the traces of subduction events can be identified by anomalies in spiciness, AOU, and POC in the mesopelagic zone (defined here as between 100 and 600 m). More importantly, these anomalous values can be distinguished by the larger scales of variability captured by a float. For instance, the Lagrangian time series of float WMO5904677 during austral spring of 2016 showed remarkable AOU and POC anomalous values at around 300 and 500 m for profiles 25 and 27. These anomalies were not associated to the seasonal shallowing of the mixed layer and were unlikely to be caused by horizontal exchanges as both AOU and POC showed strong vertical gradients along the float's trajectory. On the other hand, spiciness, which variability is not solely a result of subduction processes, showed a much higher variability at profiles 24–27. This increase in variability was likely cause to the drift of the float along the Campbell Plateau slope (south of New Zealand; black dots in Figure 1), where Polar and sub-Antarctic waters are squeezed together intensifying horizontal gradients. The resulting spiciness signal was then caused by both vertical and horizontal exchanges driven by intense dynamics circulation (Figure 2b).

In order to segregate which of these spiciness anomalies were related to subduction events, we developed a method that evaluated the presence of concomitant anomalies in spiciness and AOU, at each single profile. Our detection method only attributed an injection event if both the AOU anomaly (AOU′) and the spiciness anomaly ($\pi'$) where found at the same depth. Anomalies were defined as the difference between the measured profile (3 bin running average) and a 20 bin running average of the same profile. Given the mean vertical resolution of BGCArgo floats (between 5 and 10 m, i.e., 7.5 m mean value in the first 400 m), a 20 bin running averaged profile would smooth out features of less than 150 m in vertical extent. Previous studies have shown that the vertical scale of subducted features were of the order of 100 m or less (Omand et al., 2015; Stukel et al., 2017a, 2017b; Xu et al., 2016). Therefore, a 20 bin running average allow capturing the mean state of the profile while smoothing small-scale subducted features. A visual comparison of the 3 bin and the 20 bin smoothed signals in WMO5904677's profile 27 supports these arguments (Figure 3). In order to discard anomalous features associated to other mechanisms than subduction (for instance, horizontal cross-frontal exchanges in the mesopelagic zone), only features with strong anomalies, AOU′ $< -8$

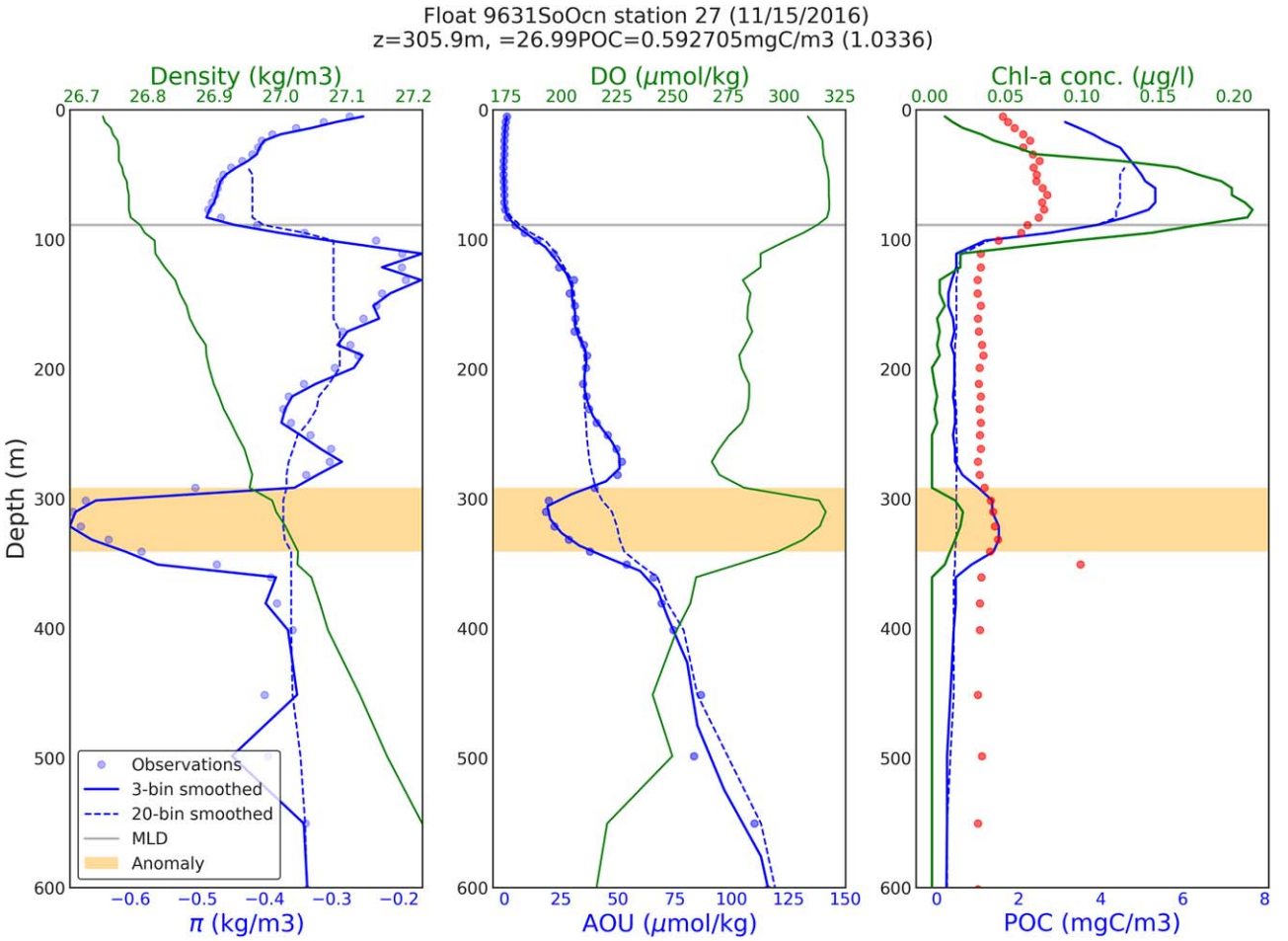


**Figure 3.** Vertical profiles of station 27 of float WMO5904677. The orange strip represents the anomalous feature identified by the detection method and defined as the upper and lower depths where AOU′ $< -1$ $\mu$mol/kg. The gray horizontal line shows the mixed-layer depth. (a) Density (green line), spiciness measurements (blue dots), 3 bin and 20 bin smoothed spiciness (solid blue and dashed blue lines, respectively). (b) DO (green line), AOU measurements (blue dots), 3 bin and 20 bin smoothed AOU (solid blue and dashed blue lines, respectively). (c) Chl-a (green line), 3 bin and 20 bin smoothed POC concentration (solid blue and dashed blue lines, respectively) and $b_{bp}$ nonsmoothed measurements (organge dots; no units).

$\mu$mol/kg and $\pi' < -0.05$, were retained. Once the event was detected based on AOU′ and $\pi'$, the POC anomaly (POC′) was used to estimate the amount of organic matter subducted. As for the rest of variables, POC′ was computed as the difference between the 3 bin and the 20 bin smoothed POC profiles (Figure 3c). Thresholds on AOU′ and $\pi'$ were chosen as the minimal values with which no false positive events were detected. This choice might have caused to not take into account some weak events (false negatives) but it ensured robustness on the events detected. Although the number of anomalies detected was found proportional to the value of AOU′ threshold, a sensitivity test showed that the average concentration of POC′ in the anomalies increased significantly for AOU′ $< -8$ $\mu$mol/kg (supporting information Figure S3).

## 3. Results

### 3.1. Float WMO5904677, Profile 27: A Case Study

In this section, we first describe a particularly strong event captured by float WMO5904677 (Figures 2 and 3). We offer here a detailed analysis of this particular profile to illustrate the validity of the method. The rest of events presented similar characteristics although with lower AOU, $\pi$ and POC anomalies.

Profile 27 of float WMO5904677 was measured south of the Campbell Plateau the 15 November 2016, during austral spring (Figure 1, black star south of New Zealand). This profile showed a relatively shallow mixed-layer depth and a significant concentration of organic matter at the surface, indicating the presence

of a phytoplankton bloom. In the mesopelagic zone, between 290 and 340 m, the float captured concomitant anomalies in spiciness ($\pi'$), AOU, DO, and POC (Figure 3). Specifically, $\pi'$ peaked at $-0.35$ kg/m$^3$, AOU′ at $-24$ $\mu$mol/kg and the highest POC concentration measured doubled the background POC concentration at the same depth. The Chl-a concentration was also significantly higher than its background value. High AOU′, $\pi'$, POC′, and Chl-a were consistently measured at seven consecutive sampling depths (at intervals of 10 m) and the thickness of the feature was close to 50 m; centered at the 27.0 kg/m$^3$ isopycnal layer. Such coherent anomalies between independent variables indicated the intrusion of a different water parcel in the water column. The very low spiciness, AOU, and salinity values (not shown) suggested that this water parcel originated in fresher (although denser) waters from the surface. The location of the event suggested that such fresher and denser waters were probably Polar Zone waters injected below Sub-Antarctic waters.

### 3.2. Spatial Distribution

The detection method was applied to 4,336 profiles in the Southern Ocean. Amongst these, 40 profiles were associated with subduction events. Seventy five percent of the events occurred in late spring and summer (supporting information Figure S2a) when subducted water is more likely to remain isolated from the surface during weeks or months without being re-entrained into the mixed layer (Dall'Olmo et al., 2016). Episodic subduction occurs throughout the year but the anomalies are easily eroded under strong winter mixing.

Events were unevenly distributed across the Southern Ocean (Figure 4). The highest concentration of events was found down-stream of the Kerguelen Plateau, while the eastern edge of the Indian Sector and the central Pacific also had a high concentration of events. Altogether, these three regions contained 70% of all detected events. The remaining 30% were scattered between the western edge of the Indian Sector and

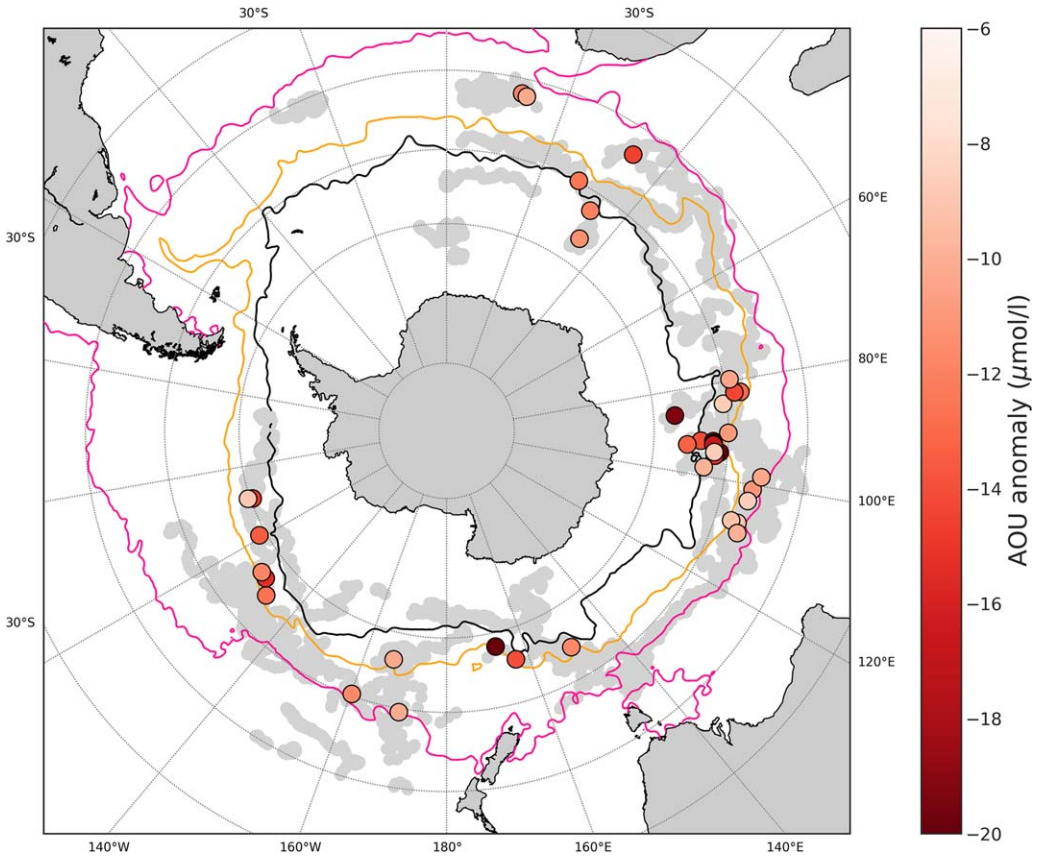


**Figure 4.** Map of the Southern Ocean showing the location of detected events (red dots) and all analyzed profiles (grey circles in the background; see Figure 1 for actual number of profiles). The value of the AOU anomaly, AOU′ (see section 2), is represented by the intensity of red color. Pink, orange, and black solid lines represent the climatological position of the STF, SAF, and PF respectively, based on Venables et al., (2012).

the vicinity of the Campbell Plateau. No events were detected north of the STF, while most events were concentrated between the SAF and the PF. Importantly, the spatial distribution of events was poorly correlated with density of profiles (Figure 1). For instance, very few events were detected in the western Indian sector or the central Pacific subtropical waters where the density of profiles was high. On the other hand, other regions with high density of profiles presented an important number of subduction events (e.g., downstream Kerguelen).

The values of AOU′ in the core of the subducted features (red color in Figure 4) ranged between −8 (minimal threshold of the detection method) and −28 $\mu$mol/kg. AOU′ was highly variable down-stream of the Kerguelen Plateau (from −8 to −20 $\mu$mol/kg) while, in other regions, like the western Indian sector and the south of the African continent, AOU′ was generally low. In frontal zones, AOU can present strong horizontal gradients (supporting information Figure S1) that could cause erroneous detections of AOU anomalies. In that case, AOU′ would only depend on the difference between water masses at each side of the front. The lack of spatial organization in the measured AOU′ showed that these anomalies were likely cause by vertical intrusions more than by horizontal exchanges.

The majority of events (90%) were found in the lee of major bathymetric features such as the Kerguelen Plateau, the South-east Indian Ridge, the Macquarie Ridge (south of the Tasman Sea), the Campbell Plateau or the Pacific-Antarctic Ridge (Figure 5a). These regions are hot spots of Eddy Kinetic Energy (EKE; Figure 5b) caused by the interaction between the Antarctic Circumpolar Current (ACC) with the bathymetry (Dufour et al., 2015; Thompson & Sallée, 2012). It is well known that these regions are rich in intense mesoscale and submesoscale jets and eddies, able to sustain sharp horizontal density gradients that induce vertical exchanges (Mahadevan, 2016; Rosso et al., 2014).

While anomalous features were detected over the full depth range of the detection method (100–600 m), the majority of events were detected between 300 and 400 m (supporting information Figure S2b). The depths of detection did not show any particular spatial pattern and in regions like Kerguelen or the East

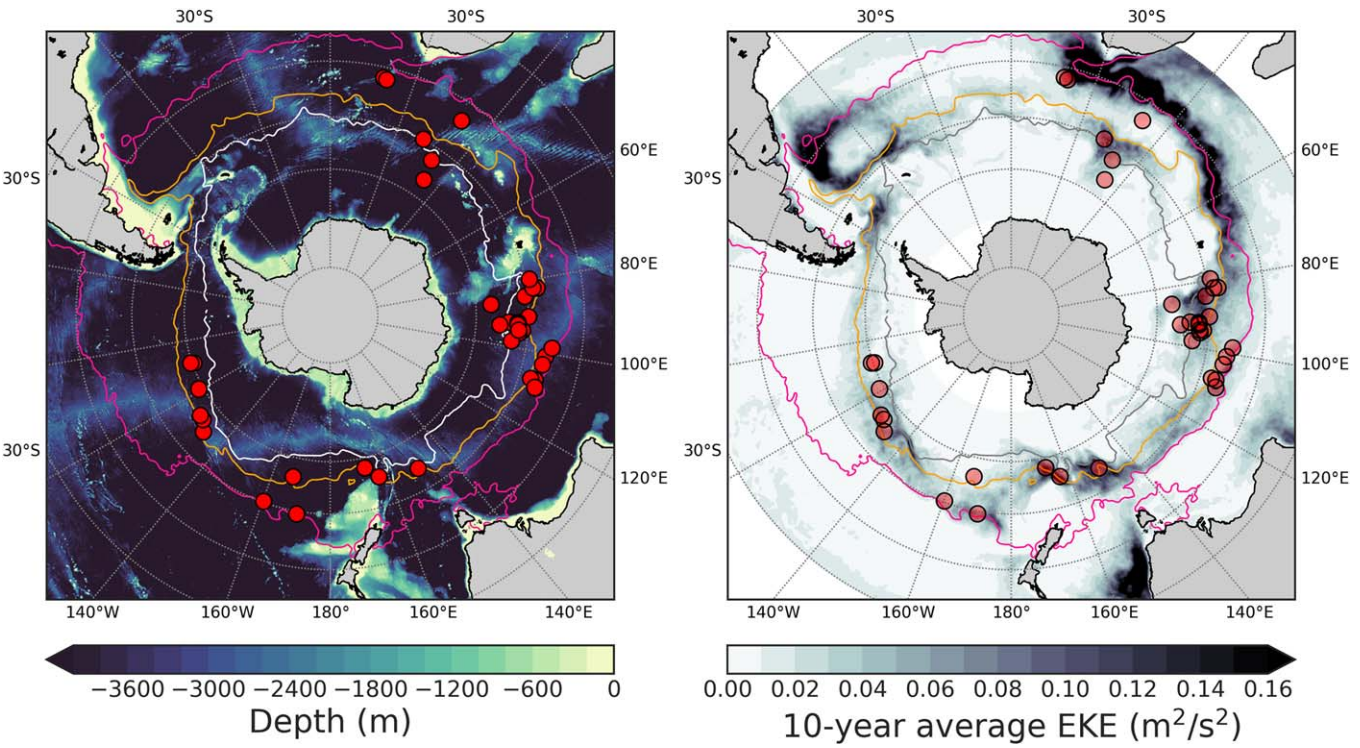


**Figure 5.** Map of the Southern Ocean showing the location of detected subduction events (red and black circles). Pink, orange/yellow and white (gray in Figure 5b) solid lines represent the climatological position of the STF, SAF, and PF, respectively, based on Venables et al. (2012). (a) Background colors represent bathymetry between 0 and 4,000 m. The major topographic features cited in the text are: the Kerguelen Plateau, between 60°E and 80°E ; the South-East Indian Ridge, at 100°E; the Macquarie Ridge, south of Tasmania (145°E); the Pacific-Antarctic Ridge, at 140°W; and the Drake Passage, at 70°W. (b) Background colors represent the 2006–2015 average eddy-kinetic energy measured by satellite (AVISO products).

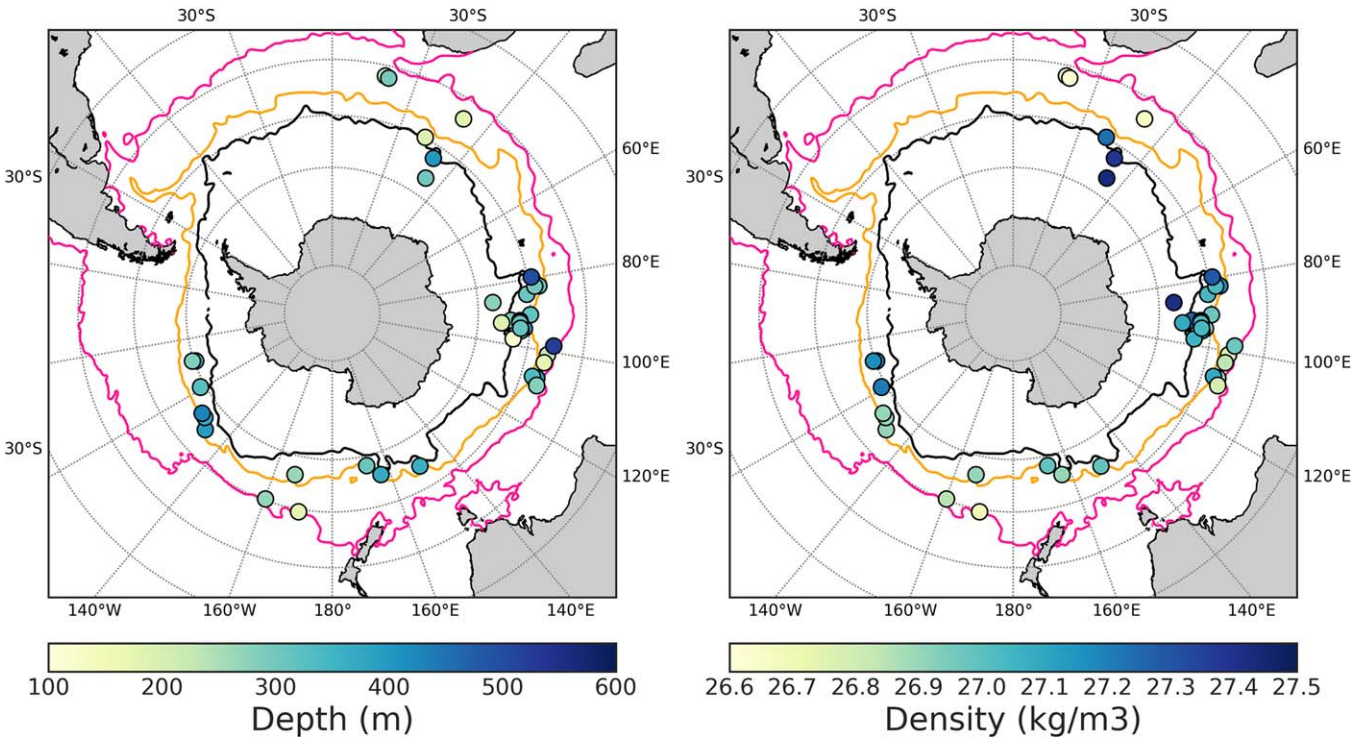


**Figure 6.** Map of the Southern Ocean showing geographical position of detected subduction events. Pink, yellow, and black solid lines represent the climatological position of the STF, SAF, and PF, respectively, based on Venables et al. (2012). (a) Circles colored by the depth at which the anomalous feature was detected. (b) Circles colored by the density at which the anomalous feature was detected.

Indian, events were detected throughout the mesopelagic zone (Figure 6a). In contrast, the density layers at which events were detected did show an organized spatial pattern across the Southern Ocean (Figure 6b). Events at the vicinity of STF were detected at densities ranging 26.6–26.9 kg/m$^3$. Between the SAF and PF they were found in denser waters, between 27 and 27.3 kg/m$^3$. Three events detected south of the PF were found in densities higher than 27.4 kg/m$^3$. Such poleward density increase is coherent with the idea that subduction events are originated in frontal systems where denser waters are subducted below less dense waters (Omand et al., 2015). Regardless of the depth at which the event was detected, the density layer carrying the subducted waters was only related to the surface waters of origin.

### 3.3. POC Concentration and Export

The optical backscattering sensors aboard BGCArgo allowed estimating the concentration of POC in the subducted features ($POC_{ev}$). $POC_{ev}$ was 0.38 mgC/m$^3$ in average with values ranging from 0.1 to 0.9 mgC/m$^3$. Compared to the background concentration of POC (i.e., 20 bin smoothed POC profile), subduction events locally increased the POC concentration to a 22%, in average. For the strongest events, $POC_{ev}$ was 2 and 3 times larger than the background concentration. High concentrations were found downstream of the Kerguelen Plateau, an iron-rich and productive region, and also in isolated events south of the Campbell Plateau and in Central Pacific (Figure 7a). Injected features held, in average, 1% of the average POC measured in the upper 50 m during the same profile ($POC_{surf}$). For the events high in POC, this value increased to 9%. These estimates must be carefully interpreted because the $POC_{surf}$ just above the event might not be representative of the POC originally contained in the subducted water.

In order to evaluate the contribution of each event to the total POC export, we estimated the vertical flux of carbon for each event as:

$$\text{Export flux} = POC_{surf} < w_{sub} > \quad (1)$$

where $<w_{sub}>$ stands for the mean vertical velocity of the injected water parcel, defined as:

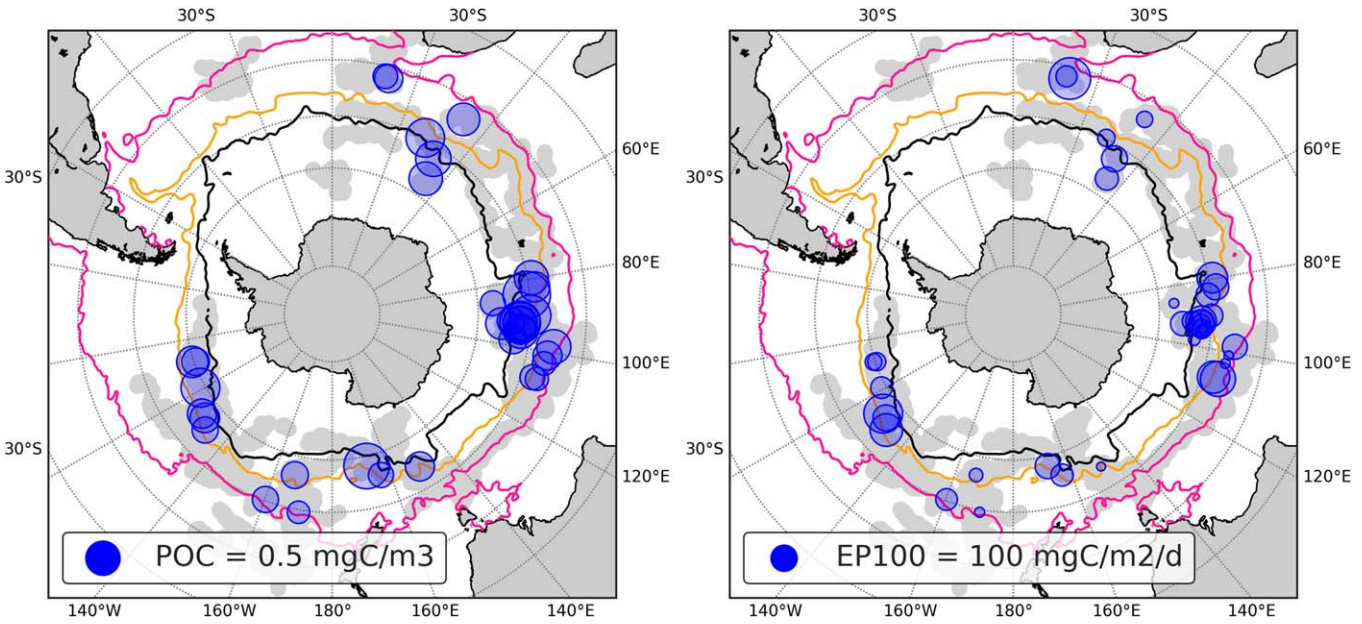


**Figure 7.** Map of the Southern Ocean showing geographical positions of subduction events. (a) Blue circles areas respresent the mean concentration of POC measured at each subudcted feature. (b) Blue circles areas represent the EP100 associated to the subduction events. Pink, red, and black solid lines represent the climatological position of the STF, SAF, and PF, respectively, based on Venables et al., (2012).

$$<w_{sub}> = (\mathrm{MLD} - \mathrm{Z_{ev}})/\Delta t \quad (2)$$

where

$$\Delta t = (\mathrm{POC_{surf}} - \mathrm{POC_{ev}})/R \quad (3)$$

R stands for the mean respiration rate of organic matter in the mesopelagic zone and is equal to 10 mmol C $m^{-3}$ $yr^{-1}$, the average respiration rate between 100 and 400 m estimated from BGCArgo floats in Southern Ocean open waters (Hennon et al., 2016). The definition of $<w_{sub}>$ in equation (2) was based on four strong assumptions:

1. $POC_{surf}$ was representative of the $POC_{ev}$ concentration in the water parcel before being subducted.
2. The difference between $POC_{surf}$ and $POC_{ev}$ was only due to respiration of organic matter since the water parcel left the surface mixed layer.
3. The distance traveled by the water parcel since leaving the mixed layer until being detected was equivalent to the difference between the depth of detection and the MLD estimated for each profile.
4. The average respiration rate in the water parcel was constant in the water parcel.

Estimated $<w_{sub}>$ values ranged between 1 and 30 m $d^{-1}$, with an average of 8 m $d^{-1}$. These values are within the range of submesoscale-induced vertical velocities (Klein & Lapeyre, 2009; Legal et al., 2007). High values were found in late summer, when most events were detected, and the spatial distribution did not show any particular pattern: all three hot spots were characterized by events with low and high export (Figure 7b). The estimated export flux was referenced at 100 m (EP100) using a Martin's curve with b = 0.5 (Buesseler et al., 2007). On average, EP100 was 62.45 gC $m^{-2}$ $yr^{-1}$ with a standard deviation of 50.49 gC $m^{-2}$ $yr^{-1}$ and values ranging from 10 to 225 gC $m^{-2}$ $yr^{-1}$. These values compare well with Henson et al. (2011) satellite estimates for high-export regions of the Southern Ocean (Figure 2b in their paper). However, little correspondence was found comparing each event EP100 to the concomitant satellite-estimated export. In order to estimate the potential contribution of these events to the POC export, we selected only the events found down-stream of Kerguelen (between 75°E and 105°E) and we compared them to field-based estimates using $^{234}Th$ and biogenic particulate Ba approaches (Jacquet et al., 2008, 2015; Planchon et al., 2015). During spring, the four events detected in this region exported 12.40 mgC $m^{-2}$ $d^{-1}$ on average, although one specific event exported 121.38 mgC $m^{-2}$ $d^{-1}$. The field-based estimates during the same period (Jacquet et al., 2008; Savoye et al., 2008) found an average flux of 104 mgC $m^{-2}$ $d^{-1}$. Therefore, in

spring, events might contribute to approximately 1% to the carbon export, although such contribution could rise up to 100% or more, for particularly strong events. On the other hand, the average export driven by late summer events was 59.15 mgC $m^{-2}$ $d^{-1}$, and field-estimates ranged between 233 and 316 mgC $m^{-2}$ $d^{-1}$ (Planchon et al., 2015). Summer events might then play a large role in carbon export, with contributions between 18% and 25%; rising up to 40% for strong events.

## 4. Discussion and Conclusion

During the last decade a number of studies have addressed the importance of mesoscale and submesoscale processes in shaping ocean biogeochemistry (Klein & Lapeyre, 2009; Mahadevan, 2016; McGillicuddy, 2016). Recent observational works have emphasized the impacts of these scales on the biological carbon pump (Omand et al., 2015; Ruiz et al., 2009; Stukel et al., 2017a, 2017b). These studies relied on heavily instrumented surveys to observe and quantify single events of organic matter subduction induced by intense ocean circulation in contrasting ocean environments. Yet, the importance of these events on the large-scale capacity of the ocean to sequester atmospheric carbon is still far from being fully quantified, both spatially and temporally.

To explore this, we developed an automated methodology to identify subduction events throughout an ocean basin. Here we used the recently created BGCArgo database in the Southern Ocean (>4,000 profiles; Figure 1) to observe mesopelagic anomalies in spiciness, AOU and POC associated to subduction events (Figures 2 and 3). This methodology allowed, for the first time, to map the occurrence of subduction events over the Southern Ocean (Figure 4). Events were not strongly correlated with the data coverage but located in three specific regions: down-stream the Kerguelen Plateau, the South-East Indian Ridge and the Pacific-Antarctic Ridge (Figure 5a). These three topographical features are known to destabilize the ACC generating hot spots of EKE in its eastern flank (Thompson & Sallée, 2012). The large amount of EKE in these regions takes the form of numerous mesoscale and submesoscale eddies and jets (Rosso et al., 2015). These structures are able to create sharp horizontal buoyancy gradients sustained by strong horizontal and vertical velocities. We argue then that the vertical velocities induced by small-scale circulation are the drivers behind the detected subduction events. Although our approach could not resolve whether subduction was caused by surface mesoscale or submesoscale circulation, the high concentration of events in submesoscale rich regions and the strong vertical velocities estimated from our data (>10 m $d^{-1}$) suggested that at least a third of the events were caused by submesocale circulation. While this conclusion agrees well with the single events previously observed (Naveira Garabato et al., 2001; Ruiz et al., 2009), our results also suggest that subduction events only take place in small regions of very intense dynamics (Figure 5b).

The vertical extent, magnitude of AOU′, and density layer at which the anomalies were detected (Figures 3, 4, and 6) allowed us to discard potential false detections resulting from the presence of recently oxygenated mode waters in the water column. More importantly, optical backscattering sensors onboard of the floats permitted estimation of the amount of organic matter vertically advected by these events (Figure 7). In particular, we estimated the POC export flux induced by these events using only the data provided by each profile. We found a large variability of the export flux of POC at 100 m, with the strongest export occurring in late summer and annual averaged values similar to satellite estimates (62.45 gC $m^{-2}$ $yr^{-1}$). In order to evaluate the importance of these events for the net export of organic matter in the Southern Ocean, we compared our estimates with previous estimates and in situ measurements in the Kerguelen region. This comparison suggested that, where detected, the contribution of episodic subduction to the total POC export flux ranged between 1% in spring, and 14–19% in summer. These contributions are significantly lower than Omand et al. (2015) estimates for the Southern Ocean. Our results also showed some extremely strong events where the estimated export was as important as sinking. Although rare and short in duration, these strong subduction events may play an important role on regularly feeding mesopelagic ecosystems in productive and high-EKE regions, such as in the lee of the Kerguelen plateau. It is worth noting that our estimates might be biased low because we used a mesopelagic respiration rate in equation (3). Sensitivity tests using surface respiration rates (Arístegui et al., 2002) resulted in export estimates 1.5–25 times larger. However, it is unclear that surface remineralization rates are appropriated for episodic subduction as we are still far to understand how fast changes in temperature and pressure may impact the microbial community.

At a large scale, episodic subduction was only detected in very specific regions of intense submesoscale circulation. Such discontinuous spatial distribution strongly contrasts with Omand et al. (2015) model-based estimates, where episodic subduction covered large areas of the Southern Ocean (Figure 4a in their paper). It also contrasts with the steady state estimates by Stuckel and Ducklow (2017), although their estimates included all vertical transport mechanisms. Our results suggest then that the average contribution of episodic subduction over the total Southern Ocean biological carbon pump might have been overestimated but more spatial and temporal coverage is needed to fully support this statement. The large variability on the carbon export caused by subduction events highlights the difficulty to extrapolate observations of a single event to basin-scale, and stresses the importance of combining local observations with large-scale observational programs.

Our study provides an innovative approach to observe the location, prevalence, and magnitude of subduction events that will be naturally improved with the continuing increase on BGCArgo measurements. In the near future, we expect to have a better spatial coverage of the Southern Ocean and thousands more measurements. These observations will help us evaluate the occurrence of subduction events in regions such as the Eastern Pacific or the Drake Passage that could not be addressed here. Although the quasi-Lagrangian nature of BGCArgo floats tends to oversample regions where floats are retained due to low mean velocities or high EKE, and to under-sample regions of high velocities (Drake Passage, for instance); strategic float deploy and sampling strategies may be able to reduce current data gaps.

The new measurements acquired by BGCArgo floats provide a whole new perspective on the small-scale vertical exchanges in the ocean. In particular, oxygen and optical backscatter were extraordinarily useful to quantify the amount of POC transported below the mixed layer. Although the 1-D nature of profiling floats data did not fully capture the 3-D pathways of subduction, it was possible to provide carbon export values that fell within the uncertainties of modeling, satellite, and in situ export current estimates. In order to reduce these uncertainties it is crucial to evaluate how eddy-pump induced export interacts with other biological pump mechanisms such as sinking of particles (Boyd & Trull, 2007) or the mixed-layer pump (Dall'Olmo et al., 2016). Multidisciplinary approaches will be needed to combine biogeochemical measurements with high-resolution satellite altimetry (SWOT) and ship-based lagrangian sampling strategies (Pascual et al., 2017; Petrenko et al., 2017). In this regard, projects such as GOCART (http://projects.noc.ac.uk/gocart/), COMICS (Sanders et al., 2016) or EXPORTS (Siegel et al., 2016) will provide excellent frameworks to quantify the different processes involved, but the BGCArgo network will still be critical to extrapolate these results to climate-relevant scales.

**Acknowledgments**

The altimeter products were produced by Ssalto/Duacs and distributed by AVISO, with support from CNES (http://www.aviso.altimetry.fr/duacs/). *Biogeochemical Argo data were collected and made freely available by the SOCCOM project (funded by NSF PLR - 1425989), remOcean project (funded by the European Research Council, GA 246777) and the SOCLIM project (funded by BNP Paribas, ENS, UPMC and CNRS).* We are extremely grateful to the teams, marine crews, and institutions who support these projects because they provide a unique set of reliable and precious data easily accessible by anyone. The authors acknowledge the insightful comments made by the two anonymous reviewers, as well as the fruitful comments and discussions with P. Boyd and M. Bressac during the creation of this document.

## References

Arístegui, J., Denis, M., Almunia, J., & Montero, M. F. (2002). Water-column remineralization in the Indian sector of the Southern Ocean during early spring. *Deep Sea Research, Part I*, *49*, 1707–1720. https://doi.org/10.1016/S0967-0645(02)00008-5

Boyd, P. W., & Trull, T. W. (2007). Understanding the export of biogenic particles in oceanic waters: Is there consensus? *Progress in Oceanography*, *72*, 276–312. https://doi.org/10.1016/j.pocean.2006.10.007

Briggs, N., Perry, M. J., Cetinić, I., Lee, C., D'asaro, E., Gray, A. M., et al. (2011). High-resolution observations of aggregate flux during a subpolar North Atlantic spring bloom. *Deep Sea Research, Part I*, *58*, 1031–1039. https://doi.org/10.1016/j.dsr.2011.07.007

Buesseler, K. O., Lamborg, C. H., Boyd, P. W., Lam, P. J., Trull, T. W., Bidigare, R. R., et al. (2007). Revisiting carbon flux through the Ocean's twilight zone. *Science*, *316*, 567–570. https://doi.org/10.1126/science.1137959

Claustre, H., & Johnson, K. (2016). The scientific rationale, design and implementation plan for a Biogeochemical-Argo float array. *Biogeochemical-Argo Planning Group*. https://doi.org/10.13155/46601

Dall'Olmo, G., Dingle, J., Polimene, L., Brewin, R. J. W., & Claustre, H. (2016). Substantial energy input to the mesopelagic ecosystem from the seasonal mixed-layer pump. *Nature Geoscience*, *9*(11), 820–823. https://doi.org/10.1038/ngeo2818

Dufour, C. O., Griffies, S. M., de Souza, G. F., Frenger, I., Morrison, A. K., Palter, J. B., et al. (2015). Role of mesoscale eddies in cross-frontal transport of heat and biogeochemical tracers in the Southern Ocean. *Journal of Physical Oceanography*, *45*, 3057–3081. https://doi.org/10.1175/JPO-D-14-0240.1

Flament, P. (2002). A state variable for characterizing water masses and their diffusive stability: Spiciness. *Progress in Oceanography*, *54*, 493–501. https://doi.org/10.1016/S0079-6611(02)00065-4

Garcia, H. E., & Gordon, L. I. (1992). Oxygen solubility in seawater: Better fitting equations. *Limnology and Oceanography*, *37*, 1307–1312. https://doi.org/10.4319/lo.1992.37.6.1307

Gille, S. T., Speer, K., Ledwell, J. R., & Naveira Garabato, A. C. (2007). Mixing and stirring in the Southern Ocean. *Eos Transactions AGU*, *88*, 382–383. https://doi.org/10.1029/2007EO390002

Haëntjens, N., Boss, E., & Talley, L. D. (2017). Revisiting Ocean Color algorithms for chlorophyll *a* and particulate organic carbon in the Southern Ocean using biogeochemical floats: REVISITING OC chl *a* AND POC IN THE SO. *Journal of Geophysical Research: Oceans*, *122*, 6583–6593. https://doi.org/10.1002/2017JC012844

Hennon, T. D., Riser, S. C., & Mecking, S. (2016). Profiling float-based observations of net respiration beneath the mixed layer. Global Biogeochem. *Global Biogeochemical Cycles*, *30*, 920–932. https://doi.org/10.1002/2016GB005380

Henson, S. A., Sanders, R., Madsen, E., Morris, P. J., Le Moigne, F., & Quartly, G. D. (2011). A reduced estimate of the strength of the ocean's biological carbon pump: Biological carbon pump strength. *Geophysical Research Letters*, *38*, L04606. https://doi.org/10.1029/2011GL046735

Huan, R. X. (2011). Defining the spicity. *Journal of Marine Research*, *69*(4–5), 545–559.

Jacquet, S. H. M., Dehairs, F., Lefèvre, D., Cavagna, A. J., Planchon, F., Christaki, U., et al. (2015). Early spring mesopelagic carbon remineralization and transfer efficiency in the naturally iron-fertilized Kerguelen area. *Biogeosciences*, *12*, 1713–1731. https://doi.org/10.5194/bg-12-1713-2015

Jacquet, S. H. M., Dehairs, F., Savoye, N., Obernosterer, I., Christaki, U., Monnin, C., et al. (2008). Mesopelagic organic carbon remineralization in the Kerguelen Plateau region tracked by biogenic particulate Ba. *Deep Sea Research, Part II*, *55*, 868–879. https://doi.org/10.1016/j.dsr2.2007.12.038

Key, R. M., Kozyr, A., Sabine, C. L., Lee, K., Wanninkhof, R., Bullister, J. L., et al. (2004). A global ocean carbon climatology: Results from Global Data Analysis Project (GLODAP): Global ocean carbon climatology. *Global Biogeochemical Cycles*, *18*, GB4031. https://doi.org/10.1029/2004GB002247

Killworth, P. D., & Hughes, C. W. (2002). The Antarctic Circumpolar Current as a free equivalent-barotropic jet. *Journal of Marine Research*, *60*, 19–45.

Klein, P., & Lapeyre, G. (2009). The oceanic vertical pump induced by mesoscale and submesoscale turbulence. *Annual Review of Marine Science*, *1*, 351–375. https://doi.org/10.1146/annurev.marine.010908.163704

Koch-Larrouy, A., Morrow, R., Penduff, T., & Juza, M. (2010). Origin and mechanism of Subantarctic Mode Water formation and transformation in the Southern Indian Ocean. *Ocean Dynamics*, *60*, 563–583. https://doi.org/10.1007/s10236-010-0276-4

Legal, C., Klein, P., Treguier, A.-M., & Paillet, J. (2007). Diagnosis of the vertical motions in a mesoscale stirring region. *Journal of Physical Oceanography*, *37*, 1413–1424. https://doi.org/10.1175/JPO3053.1

Lévy, M., Bopp, L., Karleskind, P., Resplandy, L., Ethe, C., & Pinsard, F. (2013). Physical pathways for carbon transfers between the surface mixed layer and the ocean interior. *Global Biogeochemical Cycles*, *27*, 1001–1012. https://doi.org/10.1002/gbc.20092

Mahadevan, A. (2016). The impact of submesoscale physics on primary productivity of plankton. *Annual Review of Marine Science 8*, 161–184. https://doi.org/10.1146/annurev-marine-010814-015912

McDougall, T. J., & Krzysik, O. A. (2015). Spiciness. *Journal of Marine Research*, *73*, 141–152. https://doi.org/10.1357/002224015816665589

McGillicuddy, D. J. (2016). Mechanisms of physical-biological-biogeochemical interaction at the oceanic mesoscale. *Annual Review of Marine Science 8*, 125–159. https://doi.org/10.1146/annurev-marine-010814-015606

Naveira Garabato, A. C. N., Leach, H., Allen, J. T., Pollard, R. T., & Strass, V. H. (2001). Mesoscale subduction at the Antarctic Polar Front driven by baroclinic instability. *Journal of Physical Oceanography*, *31*, 2087–2107. https://doi.org/10.1175/1520-0485(2001)031<2087:MSATAP>2.0.CO;2

Ollitrault, M., & Rannou, J.-P. (2013). ANDRO: An Argo-based deep displacement dataset. *Journal of Atmospheric and Oceanic Technology*, *30*, 759–788. https://doi.org/10.1175/JTECH-D-12-00073.1

Omand, M. M., D'asaro, E. A., Lee, C. M., Perry, M. J., Briggs, N., Cetinić, I., et al. (2015). Eddy-driven subduction exports particulate organic carbon from the spring bloom. *Science*, *348*, 222–225. https://doi.org/10.1126/science.1260062

Pascual, A., Ruiz, S., Olita, A., Troupin, C., Claret, M., Casas, B., et al. (2017). A multiplatform experiment to unravel meso- and submesoscale processes in an intense front (AlborEx). *Frontiers in Marine Science*, *4*, 39. https://doi.org/10.3389/fmars.2017.00039

Petrenko, A. A., Doglioli, A. M., Nencioli, F., Kersalé, M., Hu, Z., & D'ovidio, F. (2017). A review of the LATEX project: Mesoscale to submesoscale processes in a coastal environment. *Ocean Dynamics*, *67*, 513–533. https://doi.org/10.1007/s10236-017-1040-9

Planchon, F., Ballas, D., Cavagna, A.-J., Bowie, A. R., Davies, D., Trull, T., et al. (2015). Carbon export in the naturally iron-fertilized Kerguelen area of the Southern Ocean based on the $^{234}$Th approach. *Biogeosciences*, *12*, 3831–3848. https://doi.org/10.5194/bg-12-3831-2015

Rosso, I., Hogg, A. M., Kiss, A. E., & Gayen, B. (2015). Topographic influence on submesoscale dynamics in the Southern Ocean. *Geophysical Research Letters*, *42*, 1139–1147. https://doi.org/10.1002/2014GL062720

Rosso, I., Hogg, A. M., Strutton, P. G., Kiss, A. E., Matear, R., Klocker, A., et al. (2014). Vertical transport in the ocean due to sub-mesoscale structures: Impacts in the Kerguelen region. *Ocean Modelling*, *80*, 10–23. https://doi.org/10.1016/j.ocemod.2014.05.001

Ruiz, S., Pascual, A., Garau, B., Pujol, I., & Tintoré, J. (2009). Vertical motion in the upper ocean from glider and altimetry data. *Geophysical Research Letters*, *36*, L14607. https://doi.org/10.1029/2009GL038569

Sabine, C. L., Feely, R. A., Gruber, N., Key, R. M., Lee, K., Bullister, J. L., et al. (2004). The oceanic sink for anthropogenic $CO_2$. *Science*, *305*, 367–371. https://doi.org/10.1126/science.1097403

Sallée, J.-B., Matear, R. J., Rintoul, S. R., & Lenton, A. (2012). Localized subduction of anthropogenic carbon dioxide in the Southern Hemisphere oceans. *Nature Geoscience*, *5*, 579–584. https://doi.org/10.1038/ngeo1523

Sanders, R. J., Henson, S. A., Martin, A. P., Anderson, T. R., Bernardello, R., Enderlein, P., et al. (2016). Controls over ocean mesopelagic interior carbon storage (COMICS): Fieldwork, synthesis, and modeling efforts. *Frontiers in Marine Science*, *3*, 136. https://doi.org/10.3389/fmars.2016.00136

Sarmiento, J. L., & Gruber, N. (2006). *Ocean biogeochemical dynamics*. Princeton, NJ: Princeton University Press.

Savoye, N., Trull, T. W., Jacquet, S. H. M., Navez, J., & Dehairs, F. (2008). 234Th-based export fluxes during a natural iron fertilization experiment in the Southern Ocean (KEOPS). *Deep Sea Research, Part II*, *55*, 841–855. https://doi.org/10.1016/j.dsr2.2007.12.036

Siegel, D. A., Buesseler, K. O., Behrenfeld, M. J., Benitez-Nelson, C. R., Boss, E., Brzezinski, M. A., et al. (2016). Prediction of the export and fate of global ocean net primary production: The EXPORTS science plan. *Frontiers in Marine Science*, *3*, 22. https://doi.org/10.3389/fmars.2016.00022

Spall, M. A. (1995). Frontogenesis, subduction, and cross-front exchange at upper ocean fronts. *Journal of Geophysical Research*, *100*, 2543–2557. https://doi.org/10.1029/94JC02860

Stukel, M. R., Aluwihare, L. I., Barbeau, K. A., Chekalyuk, A. M., Goericke, R., Miller, A. J., et al. (2017a). Mesoscale ocean fronts enhance carbon export due to gravitational sinking and subduction. *Proceedings of the National Academy of Sciences of United States of America*, *114*, 1252–1257. https://doi.org/10.1073/pnas.1609435114

Stukel, M. R., & Ducklow, H. W. (2017). Stirring up the biological pump: Vertical mixing and carbon export in the Southern Ocean. *Global Biogeochemical Cycles*, *231*, 1420–1434. https://doi.org/10.1002/2017GB005652

Stukel, M. R., Song, H., Goericke, R., & Miller, A. J. (2017b). The role of subduction and gravitational sinking in particle export, carbon sequestration, and the remineralization length scale in the California Current Ecosystem. *Limnology and Oceanography Methods*, *63*, 363–383. https://doi.org/10.1002/lno.10636

Thompson, A. F., & Sallée, J.-B. (2012). Jets and topography: Jet TRANSITIONS AND THE IMPACT ON TRANsport in the Antarctic circumpolar current. *Journal of Physical Oceanography*, *42*, 956–972.

Turner, J., Bindschadler, R., Convey, P., DiPrisco, G., Fahrbach, E., Gutt, J., et al. (Eds.) (2009). Antarctic climate change and the environment: A contribution to the International Polar Year 2007–2008. Cambridge, UK: Scientific Committee on Antarctic Research.

Venables, H., Meredith, M. P., Atkinson, A., & Ward, P. (2012). Fronts and habitat zones in the Scotia Sea. *Deep Sea Research, Part II*, *59–60*, 14–24. https://doi.org/10.1016/j.dsr2.2011.08.012

Watson, A. J., Meredith, M. P., & Marshall, J. (2014). The Southern Ocean, carbon and climate. *Philosophical Transactions of the Royal Society A*, *372*, 20130057. https://doi.org/10.1098/rsta.2013.0057

Williams, R. G. (2001). Ocean Subduction. In J. H. Steele, K. K. Turekian, & S. A. Thorpe (Eds.), *Encyclopedia of Ocean Sciences* (pp. 1982–1993). New York, NY: Elsevier.

Xu, L., Li, P., Xie, S.-P., Liu, Q., Liu, C., & Gao, W. (2016). Observing mesoscale eddy effects on mode-water subduction and transport in the North Pacific. *Nature Communications*, *7*, 10505. https://doi.org/10.1038/ncomms10505

Xu, L., Xie, S.-P., McClean, J. L., Liu, Q., & Sasaki, H. (2014). Mesoscale eddy effects on the subduction of North Pacific mode waters. *Journal of Geophysical Research: Oceans*, *119*, 4867–4886. https://doi.org/10.1002/2014JC009861